Contents list available at IJRED website

International Journal of Renewable Energy Development

Journal homepage: https://ijred.undip.ac.id

Research Article

3D Numerical Investigation of Free Convection using Lattice Boltzmann and Finite Difference Methods

Jaouad Benhamou*, El Bachir Lahmer, Mohammed Jami, Mohammed Amine Moussaoui, Ahmed Mezrhab

Laboratory of Mechanics & Energetics, Faculty of Sciences, Mohammed First University 60000 Oujda, Morocco

Abstract. Numerical study of various physical phenomena in three dimensions has become a necessity to better understand the physical process than in two dimensions. Thus, in this paper, the code is elaborated to be adapted to the simulation of heat transfer in three dimensions. The numerical simulations are performed using a hybrid method. This method is based on the lattice Boltzmann approach for the computation of velocities, and on the finite difference technique for the calculation of temperature. The used numerical code is validated by examining the free convection in a cubic enclosure filled with air. Then, the analysis of the heat exchange between two cold vertical walls and a heated block located at the center of a cubic cavity is considered. The performed simulations showed that for a small value of the Rayleigh number ($Ra=10^3$ for example), the fluid exchanges its heat almost equally with all hot surfaces of the obstacle. However, for large values of Ra ($Ra \geq 10^4$), the numerical results found showed that the heat exchange rate is greater on the bottom face compared to the other faces of the obstacle.

Keywords: Lattice Boltzmann method; Finite difference method; Hybrid method; Free convection, Fluid flow, 3D simulation

Received: 23rd March 2022; Revised: 5th June 2022; Accepted: 16th June 2022; Available online: 27th June 2022

1. Introduction

Heat transfer or thermal transfer is a transit of energy in a disordered microscopic form. It occurs as a result of a complex interaction in or between environments with different temperatures. It is widely present in nature and many industrial sectors. There are generally three main modes of heat transfer such as conduction, convection, and radiation. Convection is a heat exchange that takes place through the movement of matter in a liquid or gaseous medium. Thermal conduction is the transfer of internal energy by microscopic diffusion and collisions of molecules, atoms, and electrons. Heat transfer by radiation is caused by electromagnetic radiation, called thermal radiation (Minkowycz *et al*., 2000; Bejan & Kraus, 2003).

In 2D, Karki *et al*. (2019) numerically studied the effect of adiabatic blocks on free convection in a square cavity. For the case of a block in the center of the cavity, they found that the average heat transfer increases along the hot surface with increasing block size until reaching an optimal value. Then, with a further increase in size, the heat transfer rate degrades. They also found that the presence of obstacles outside the central conduction zone decreases the heat exchange despite the adiabatic nature of the obstacles. Nouni *et al*. (2021) studied the effect of obstacles on the natural convection inside a differentially heated square cavity using the lattice Boltzmann method. Xiong *et al*. (2021) performed numerical simulations of mixed convection flow and heat transfer in a lid-driven triangular cavity with different obstacle configurations. Khan *et al*. (2021) analyzed the natural non-equilibrium thermal convection in a trapezoidal porous enclosure. They introduced heated cylindrical obstacles inside the cavity to examine the thermal behavior. Subhani & Kumar (2021) examined the improvement of heat transfer by free convection of a circular obstacle in a square cavity. Yousif *et al*. (2022) studied the effect of using triple adiabatic blocks on free convection inside a porous enclosure.

In 3D, Ghachem *et al*. (2018) numerically examined the free convection and entropy generation in a cubic cavity equipped with a baffle. In particular, they analyzed the influence of the position and thickness of the baffle on the hydrodynamic and thermal behaviors of the fluid studied. Lee (2018) studied the effect of the presence of an obstacle placed in the middle of a parallele piped enclosure on the Rayleigh-Benard natural convection. Purusothaman *et al*. (2019) performed a 3D study of free convection heat exchange from a variable solid rectangular heat source. Chorin *et al*. (2020) experimentally studied a natural convection flow in a differentially heated cavity in the presence of a localized obstacle. They analyzed the influence of length and vertical position for an insulating and a conducting obstacle. Vesper *et al*. (2022) analyzed the influence of horizontal conductive walls and conductive fins on free air convection in laterally heated enclosures.

* Corresponding author:
Email: jaouad1994benhamou@gmail.com (J. Benhamou)

https://doi.org/10.14710/ijred.2022.45383
ISSN: 2252-4940/© 2022.The Author(s). Published by CBIORE

Ugurlubilek *et al.* (2022) numerically studied the laminar free convection heat transfer in differentially heated air-filled cubic cavities with partitions attached to the walls at different positions.

This paper proposes a hybrid numerical method to study the natural convection in 3D between two cold sidewalls of a cubic cavity and a hot obstacle located at its center. This method is composed of two different approaches. The first one is the mesoscopic lattice Boltzmann approach and the second one is the macroscopic finite difference technique. Indeed, the association of these methods is commonly used in two dimensions to analyze different thermal systems in various geometries (Lallemand & Luo, 2003; Shi *et al.*, 2006; Xu *et al.*, 2006; Bettaibi *et al.*, 2014; Hasnaoui *et al.*, 2018). In three dimensions, FDM methods have been used for many years to perform various numerical simulations, while the LBM approach is relatively new. Their coupling in 3D has recently started, in particular the coupling between FDM and LBM-SRT (Liu *et al.*, 2018; Nee, 2020a, 2020b, 2021). In this work, a more accurate hybrid model is chosen to study the dynamic and thermal behaviors of air inside an air-filled 3D cavity. It concerns the implementation of the LBM-MRT model with the FDM technique based on the fourth-order central scheme.

The LBM and FDM numerical methods are applied at two different levels of description. Indeed, the LBM is founded on statistical calculations. It has been developed very significantly since the early 2000s. It is based on the computation of the velocity distribution of molecules. The usual quantities are then deduced by calculating the moments of the velocity distribution. This approach can be seen as a discretization of the Boltzmann equation, which corresponds to the probability density of the velocities of the molecules in a diluted gas over an infinitesimal volume (Mohamad, 2019). On the other hand, finite difference methods are a class of numerical techniques for solving differential equations by approximating derivatives with finite differences. The spatial domain and time interval are discretized or divided into a finite number of steps, and the value of the solution at these discrete points is approximated by solving algebraic equations containing finite differences and values from adjacent points (Özişik *et al.*, 2017).

The present paper focuses on the study of free convection between a hot solid and cold walls of an air-filled cavity. The main objective of this study is to get closer to the practice of cooling electronic components by thermal convection. Here, the electronic component is represented by the hot solid. The characterization of the heat exchange between this solid and the cold air is performed by calculating the local and average Nusselt numbers. The results found and the numerical methods used to perform the simulations are discussed in the following sections.

2. Numerical methods

2.1. D3Q19-MRT lattice Boltzmann model

This paper uses the D3Q19-MRT lattice Boltzmann lattice model to calculate the velocities and density. This is performed by numerically solving the Boltzmann equation (Eq. (1)) (Benhamou *et al.*, 2020, 2022; Lahmer *et al.*, 2022; Admi *et al.*, 2022).

$$f_i(x_i + c_i\Delta t, t + \Delta t) = f_i(x_i, t) + M^{-1}S\left[m_i^{eq} - m_i\right] \quad (1)$$

The D3Q19 lattice is a three-dimensional scheme with nineteen directions of propagation of fluid particles (Figure 1). The velocities c_i of this lattice are defined in equation (2) (Benhamou & Jami, 2022; D'Humières *et al.*, 2002). m_i is a vector composed of 19 physical quantities (Eq. (3)) such as density, momentum (j_x, j_y, j_z), heat flux quantities (q_x, q_y, q_z), kinetic energy (e) and its square (e^2), and others. All the components of the vector m_i are given in detail in the references (Benhamou & Jami, 2022; D'Humières *et al.*, 2002).

The matrix S is a diagonal matrix. It is composed of 19 relaxation times s_i. Its mathematical representation is given by equation (4). The diagonal matrix S used in this study is the one used in our previous work (Benhamou & Jami, 2022). The elements s_0, s_3, s_5 and s_7 are fixed at unity ($s_0 = s_3 = s_5 = s_7 = 1$). They are related to the density ρ and the impulses j_x, j_y and j_z, respectively. The relaxation times s_9, s_{11}, s_{13}, s_{14} and s_{15} are given as a function of the LBM kinematic viscosity as $s_9 = s_{11} = s_{13} = s_{14} = s_{15} = 1/(3\nu + 0.5)$. s_1 can be set to 1.19. The other elements (s_2, s_4, s_6, s_{10}, s_{12}, s_{16}, s_{17} and s_{18}) are free parameters.

The mathematical form of the transformation matrix M is given in reference (Benhamou *et al.*, 2021). The vector m_i^{eq} can be defined from the density and the momentum by equation (5) (Li *et al.*, 2016). For the LBM method, physical quantities like density (ρ) and velocities (v_x, v_y, v_z) are determined using equation (6).

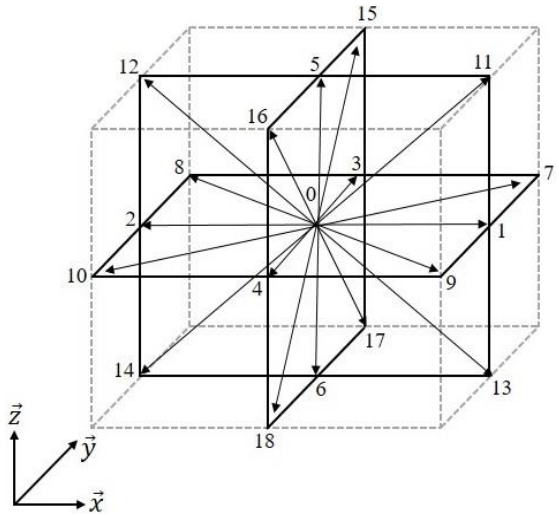

Fig 1. The D3Q19-LBM lattice.

$$c_i = c\begin{pmatrix} 0 & 1 & -1 & 0 & 0 & 0 & 0 & 1 & -1 & 1 & -1 & 1 & -1 & 1 & -1 & 0 & 0 & 0 & 0 \\ 0 & 0 & 0 & 1 & -1 & 0 & 0 & 1 & 1 & -1 & -1 & 0 & 0 & 0 & 0 & 1 & -1 & 1 & -1 \\ 0 & 0 & 0 & 0 & 0 & 1 & -1 & 0 & 0 & 0 & 0 & 1 & 1 & -1 & -1 & 1 & 1 & -1 & -1 \end{pmatrix} \quad (2)$$

$$m_i = \left(\rho, e, e^2, j_x, q_x, j_y, q_y, j_z, q_z, 3p_{xx}, 3\pi_{xx}, p_{ww}, \pi_{ww}, p_{xy}, p_{yz}, p_{zx}, m_x, m_y, m_z\right)^T \quad (3)$$

$$S = \mathrm{diag}(s_0, s_1, s_2, s_3, s_4, s_5, s_6, s_7, s_8, s_9, s_{10}, s_{11}, s_{12}, s_{13}, s_{14}, s_{15}, s_{16}, s_{17}, s_{18}) \quad (4)$$

$$\begin{array}{cccc} m_0^{eq} = \rho & m_1^{eq} = -11\rho + 19\dfrac{j_x^2 + j_y^2 + j_z^2}{\rho_0} & m_2^{eq} = 3\rho - \dfrac{11}{2}\dfrac{j_x^2 + j_y^2 + j_z^2}{\rho_0} & m_3^{eq} = j_x \\ m_4^{eq} = -\dfrac{2}{3}j_x & m_5^{eq} = j_y & m_6^{eq} = -\dfrac{2}{3}j_y & m_7^{eq} = j_z \\ m_8^{eq} = -\dfrac{2}{3}j_z & m_9^{eq} = \dfrac{2j_x^2 - \left(j_y^2 + j_z^2\right)}{\rho_0} & m_{10}^{eq} = -\dfrac{1}{2}\dfrac{2j_x^2 - \left(j_y^2 + j_z^2\right)}{\rho_0} & m_{11}^{eq} = \dfrac{j_y^2 - j_z^2}{\rho_0} \\ m_{12}^{eq} = -\dfrac{1}{2}\dfrac{j_y^2 - j_z^2}{\rho_0} & m_{13}^{eq} = \dfrac{j_x j_y}{\rho_0} & m_{14}^{eq} = \dfrac{j_y j_z}{\rho_0} & m_{15}^{eq} = \dfrac{j_x j_z}{\rho_0} \\ m_{16}^{eq} = 0 & m_{17}^{eq} = 0 & m_{18}^{eq} = 0 & \end{array} \quad (5)$$

$$\rho = \sum_{i=0}^{18} f_i\,, \quad v_{x,y,z} = \frac{1}{\rho}\sum_{i=0}^{18} f_i\, c_i \quad (6)$$

2.2 Finite difference technique based on the fourth-order central scheme

The solution of differential equations, or more generally partial differential equations, occupies an important place in engineering and applied mathematics. There are several techniques for resolving partial differential equations such as finite element methods, finite difference techniques, finite volume methods, spectral methods, and so on. The finite difference method is one of the oldest numerical simulation methods that is still used for some applications, in particular, in the field of compressible fluid mechanics.

To model free convection, the governing equations for the conservation of mass, momentum, and energy are expressed in (7-11) (Benhamou & Jami, 2022). The temperature θ can be determined from the average dimensional temperature ($T_m = (T_h + T_c)/2$), the cold temperature T_c, and the hot temperature T_h as $\theta = (T - T_m)/(T_h - T_c)$.

In this work, the FDM technique is applied to compute the temperature by resolving the macroscopic energy equation (Eq. (11). There are many finite difference schemes to give partial derivatives in the discretized form (Özişik *et al*., 2017). They can be classified according to their order of discretization. For accuracy, the fourth-order centered finite difference scheme is employed in this paper to approximate the first and second spatial derivatives given in equation (11). In the $\boldsymbol{y}$ −direction, for example, the derivatives $\boldsymbol{\partial\theta/\partial y}$ and $\boldsymbol{\partial^2\theta/\partial y^2}$ are approximated by equations (12) and (13), respectively (Benhamou & Jami, 2022).

The temporal derivative $\partial\theta/\partial t$ is given by using the forward difference approximation (Eq. (14)).

$$\frac{\partial v_x}{\partial x} + \frac{\partial v_y}{\partial y} + \frac{\partial v_z}{\partial z} = 0 \quad (7)$$

$$\rho\left(\frac{\partial v_x}{\partial t} + v_x\frac{\partial v_x}{\partial x} + v_y\frac{\partial v_x}{\partial y} + v_z\frac{\partial v_x}{\partial z}\right) = \mu\left(\frac{\partial^2 v_x}{\partial x^2} + \frac{\partial^2 v_x}{\partial y^2} + \frac{\partial^2 v_x}{\partial z^2}\right) - \frac{\partial p}{\partial x} \quad (8)$$

$$\rho\left(\frac{\partial v_y}{\partial t} + v_x\frac{\partial v_y}{\partial x} + v_y\frac{\partial v_y}{\partial y} + v_z\frac{\partial v_y}{\partial z}\right) = \mu\left(\frac{\partial^2 v_y}{\partial x^2} + \frac{\partial^2 v_y}{\partial y^2} + \frac{\partial^2 v_y}{\partial z^2}\right) - \frac{\partial p}{\partial y} \quad (9)$$

$$\rho\left(\frac{\partial v_z}{\partial t} + v_x\frac{\partial v_z}{\partial x} + v_y\frac{\partial v_z}{\partial y} + v_z\frac{\partial v_z}{\partial z}\right) = \mu\left(\frac{\partial^2 v_z}{\partial x^2} + \frac{\partial^2 v_z}{\partial y^2} + \frac{\partial^2 v_z}{\partial z^2}\right) - \frac{\partial p}{\partial z} + \rho g\beta\left(\theta - \theta_{ref}\right) \quad (10)$$

$$\frac{\partial\theta}{\partial t} + v_x\frac{\partial\theta}{\partial x} + v_y\frac{\partial\theta}{\partial y} + v_z\frac{\partial\theta}{\partial z} = \alpha\left(\frac{\partial^2\theta}{\partial x^2} + \frac{\partial^2\theta}{\partial y^2} + \frac{\partial^2\theta}{\partial z^2}\right) \quad (11)$$

$$\left(\frac{\partial\theta}{\partial y}\right)_j = \frac{\theta_{j-2} + 8\theta_{j+1} - 8\theta_{j-1} - \theta_{j+2}}{12\Delta y} + \phi(\Delta y^4) \quad (12)$$

$$\left(\frac{\partial^2\theta}{\partial y^2}\right)_j = \frac{-\theta_{j-2} + 16\theta_{j-1} - 30\theta_j + 16\theta_{j+1} - \theta_{j+2}}{12\Delta y^2} + \phi(\Delta y^4) \quad (13)$$

$$\frac{\partial\theta}{\partial t} = \frac{\theta(t + \Delta t) - \theta(t)}{\Delta t} + \phi(\Delta t) \quad (14)$$

2.3.Boundary conditions

In general, boundary conditions are very important for the stability of numerical calculations and the precision of results. They allow defining the limits of the studied geometry. In this article, two types of boundary conditions are considered.

The first is the LBM conditions to define the solid surfaces of the cubic cavity. These surfaces cause fluid backflow when it encounters them. This fluid return is adopted at the limits using the bounce-back boundary conditions (Benhamou *et al.*, 2020, 2021; Mohamad, 2019). The second type is the thermal conditions. These conditions allow specifying the adiabatic and isothermal boundaries. In this study, the adiabatic surfaces are determined by the zero spatial derivatives of the temperature θ at the boundaries ($\partial\theta/\partial n = 0$) (Benhamou & Jami, 2022). The cold surfaces are maintained at a temperature (θ_c) of -0.5. The hot walls are set at a dimensionless temperature (θ_h) of 0.5 (Mezrhab *et al.*, 2010).

Since an unsteady partial differential equation is considered to determine the temperature (energy equation), the use of initial conditions is also necessary. At the input of our LBM code, the temperature is set to θ_c at the cold walls and θ_h at the hot walls. The velocities v_x, v_y and v_z are fixed at zero (immobile walls).

3. Results and discussions

3.1. Code validation

The present hybrid numerical code is tested by studying the free convection created in a cubic cavity filled with air and heated in a differential manner. This thermal problem has been studied numerically and experimentally in 2D and 3D in the literature for many years. It has many advantages including the simplicity of the studied geometry. It is considered a well-known reference problem to validate various new numerical methods. In this document, the geometry illustrated in Figure 2 is considered. The left vertical wall is hot. Its opposite is cold. The other surfaces are adiabatic. A gravity field is present in the cavity to force the flow of fluid.

Our calculations started first with the mesh study. Several meshes were arbitrarily used to discretize the cubic cavity. Numerical tests were necessary to optimize the time and accuracy of the calculations. Table 1 shows the value of the average Nusselt number that is calculated at the central plane ($y = 0.5$) for various tested meshes and different values of Ra.

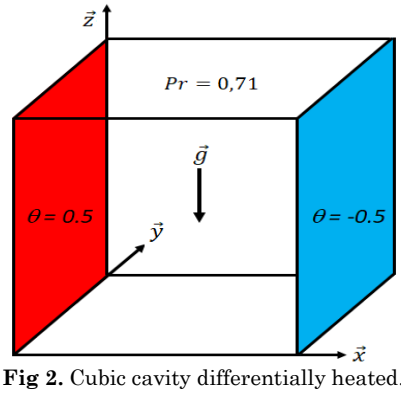

Fig 2. Cubic cavity differentially heated.

Table 1
Values of $\langle N_u \rangle$ computed at $y = 0.5$ for different meshes and different Ra.

Ra	Mesh	$\langle N_u \rangle$
10^3	$20 \times 20 \times 20$	1.151
	$40 \times 40 \times 40$	1.112
	$60 \times 60 \times 60$	1.101
10^4	$20 \times 20 \times 20$	2.421
	$40 \times 40 \times 40$	2.333
	$60 \times 60 \times 60$	2.281
10^5	$20 \times 20 \times 20$	4.867
	$40 \times 40 \times 40$	4.712
	$60 \times 60 \times 60$	4.612
10^6	$20 \times 20 \times 20$	9.301
	$40 \times 40 \times 40$	9.147
	$60 \times 60 \times 60$	8.931

To compare the $\langle Nu \rangle$ values found for each mesh, a comparison with the results obtained by Fusegi *et al.* (1991) and Wang *et al.* (2017) was performed. Table 2 illustrates this comparison. The $\langle Nu \rangle$ values found for the case of a small mesh ($20 \times 20 \times 20$) are not similar to those obtained by these references. This led us to increase the number of nodes defining the LBM lattice. For example, for the mesh 60×60×60, the results found are very close to those of the literature. This is confirmed by the low value of the relative error between our results and those of the references (Fusegi *et al.*, 1991; Wang *et al.*, 2017). Thus, it can be said that our LBM code is well validated. To further verify this validation, the temperature fields are traced in Figures 3(a) and 3(b) for low (10^3) and high (10^6) values of the Rayleigh number. The shapes of the curves obtained are similar to those found in the literature.

The average Nusselt number is computed using equation (15) (Mezrhab *et al.*, 2010; Wang *et al.*, 2017).

$$\langle N_u \rangle = -\frac{\mathrm{Lz}}{\theta_h - \theta_c}\left(\frac{\partial\theta}{\partial x}\right)_{y=0.5} \tag{15}$$

where Lz represents here the characteristic length.

3.2. Study of the heat exchange between two cold vertical walls of a cubic cavity and a hot obstacle

After validating our numerical code with reference results available in the published literature, we proceeded to the investigation of the free convection of air confined in a cubic cavity exposed to a horizontal temperature gradient. The cubic enclosure is characterized by a width Ly, a length Lx, and a height Lz. Its vertical walls located at $x = 0$ and $x = \mathrm{Lx}$ are cold and the other surfaces are assumed to be adiabatic. A hot obstacle of length lx, width ly, and height lz is placed in the center of the cavity (see Figure 4) to examine its thermal exchange with the cold surfaces. The height of the solid is equal to its length (lz = lx = Lx/5) and the width is set to Ly (ly = Ly).

Table 2
Comparison of $\langle N_u \rangle$ calculated at $y = 0.5$ for a mesh $60 \times 60 \times 60$ and different Rayleigh numbers with the literature results.

Ra	10^3	10^4	10^5	10^6
Wang *et al.* (2017)	1.088	2.247	4.599	8.779
Fusegi *et al.* (1991)	1.105	2.320	4.646	9.012
*O*ur results	1.101	2.281	4.612	8.931
Er (%) (Wang *et al.* (2017))	1.19	1.51	0.28	1.73
Er (%) (Fusegi *et al.* (1991))	0.36	1.68	0.73	0.89

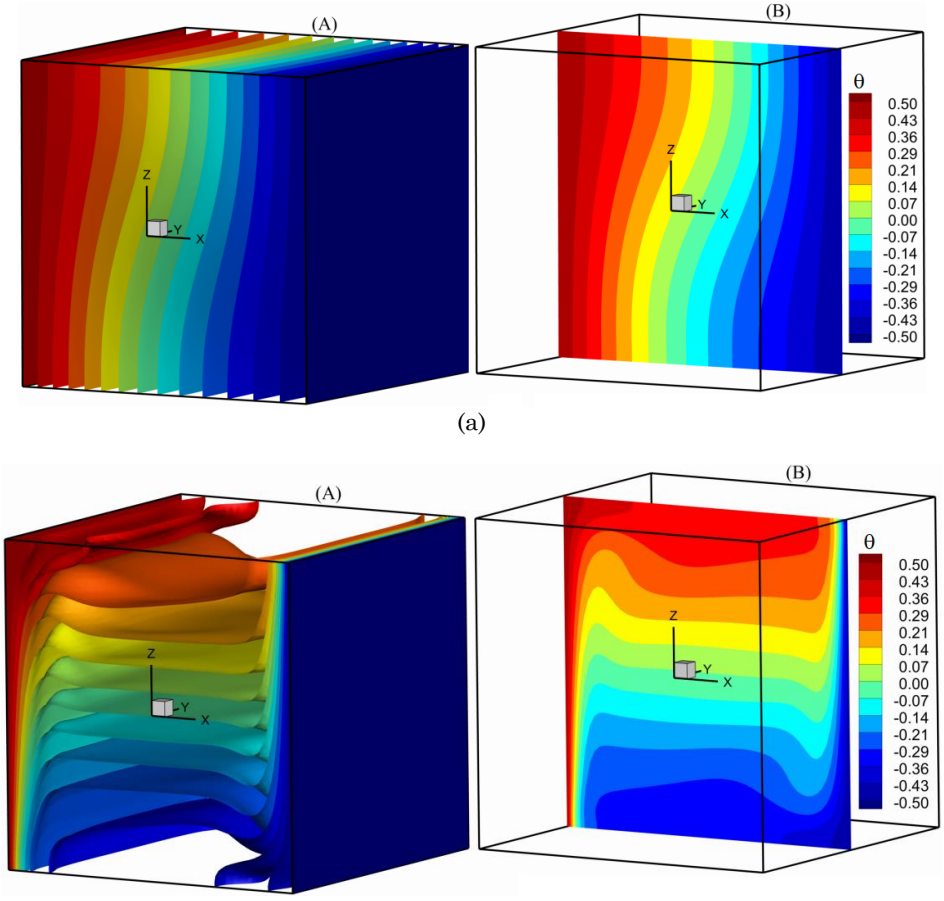

Fig 3. 3D (A) and 2D (B) representations of isotherms plotted in the cavity for $Ra = 10^3$ (a) and 10^6 (b). The 2D representation is given for a vertical section at $y = 0.5$.

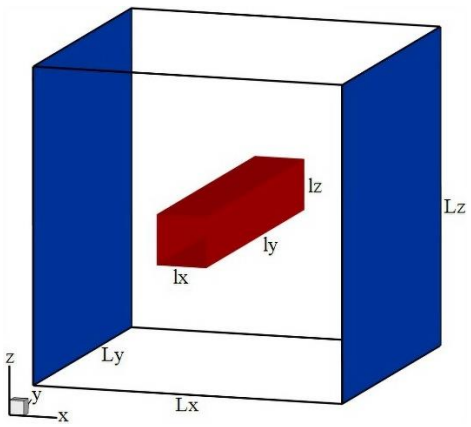

Fig 4. Illustration of the simulated thermal problem.

Numerically, to take into account the natural convection, the buoyancy force must be introduced in the LBM code. There are several models for implementing a body force in the lattice Boltzmann method (Krivovichev, 2019). The most popular and widely used models in the bibliography are the model of Shan and Chen (1993, 1994) and the model proposed by Luo (1998). The first one consists of integrating the force into the momentum. However, the second one proposes to add a discretized force (F_i) to the Boltzmann equation. In this work, the model proposed by Luo is used. Thus, the mathematical form of equation (1) becomes that given by equation (16).

$$f_i(x_i + c_i\Delta t, t + \Delta t) = f_i(x_i, t) + M^{-1}S\left[m_i^{eq} - m_i\right] + \Delta t F_i \quad (16)$$

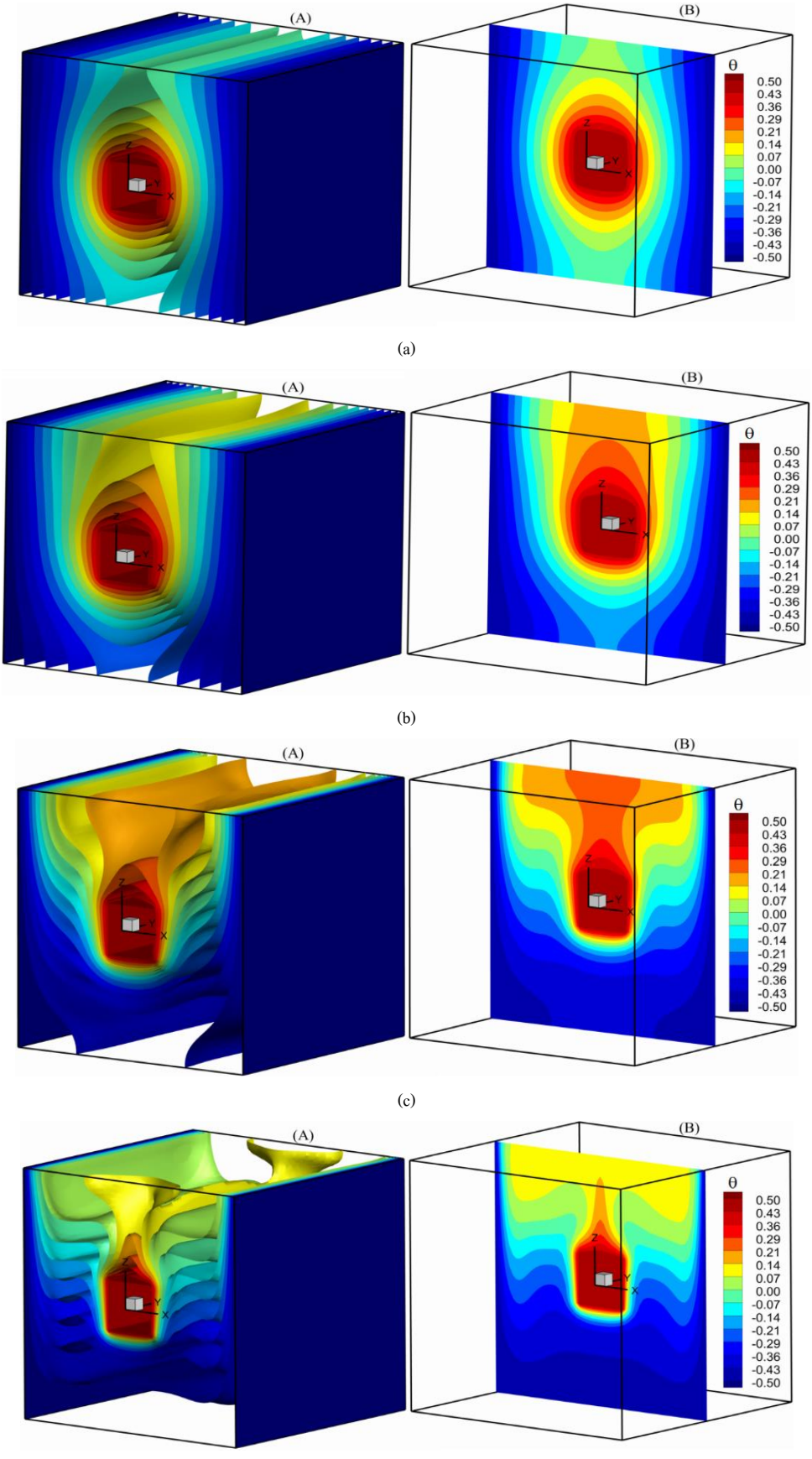

Fig 5. 3D (A) and 2D (B) representations of the temperature field for $Ra = 10^3$ (a), 10^4 (b), 10^5 (c) and 10^6 (d). The 2D representation is given for a vertical section at $y = 0.5$.

The mathematical form of the discretized force can be written as in equation (17) (Benhamou *et al.*, 2020; Mohamad & Kuzmin, 2010).

$$F_i = 3W_i c_i \rho g \beta (\theta - \theta_m) \quad (17)$$

Figure 5(a) shows the 2D (A) and 3D (B) representations of the isotherms obtained in the cavity shown in Figure 4 for a low Rayleigh number ($Ra = 10^3$). It shows that they have cylindrical shapes near the obstacle where they take maximum values. Their shapes flatten near the cold walls where they are minimal. Indeed, for $Ra = 10^3$, the free convection is weak. Therefore, the temperature is almost equally distributed upward and downward along $\vec{z}$ and -$\vec{z}$, as illustrated by the 2D temperature representation given for the vertical section at $y = 0.5$Ly. The increase in Ra modifies the shape of the temperature distribution in the cavity. For example, for $Ra = 10^4$, the temperature takes a curved shape from the top to the bottom as shown in Figure 5(b). Part of the curves becomes horizontal indicating the existence of a horizontal gradient (Figures 5(c) and (d)). Indeed, for low values of Ra ($Ra < 10^5$), the heat flows mainly by conduction inside the cavity. When Ra becomes important ($Ra \geq 10^6$), convection becomes dominant compared to conduction. The fluid in contact with the hot block heats up and rises quickly to the top. The temperature becomes significant in the upper region and is minimal below the obstacle and near the two cold faces of the cavity (Purusothaman *et al.*, 2016; Ibrahim *et al.*, 2021).

Figures 6(a)-(d) show the velocity field plotted at the center plane of the cavity ($\vec{x}, \vec{z}$) for different Rayleigh numbers. For the case of $Ra = 10^3$ and 10^4, it is clear that the fluid flows symmetrically through the cavity and it creates symmetrical recirculations on the right and left of the obstacle. When the natural convection starts to become important ($Ra = 10^5$), Figure 6(c) shows that the recirculations tend to rise towards the upper region. This is very visible in the case of $Ra = 10^6$ (Figure 6(d)). This is due to the fluid movement that becomes important in the upper zone of the cavity.

The work presented in this article can be considered as a direct application of the cooling of an electronic component which is represented here by the hot solid. To characterize the heat transfer between the block and the cold fluid, the average and local Nusselt numbers are calculated at the different faces of this obstacle. Figure 7(a) presents the evolution of Nu calculated in the middle of the left face of the obstacle. It can be noted from this figure that the rate of heat exchange increases with increasing Ra. This figure also shows that, for all Rayleigh numbers, Nu starts with a maximum value, decreases to a minimum value, and then rises again. Due to the symmetry, the heat exchange is similar for the right face and the same remark can be given. On the other hand, for the upper and lower faces, the heat exchange is not similar. Figures 7(b) and (c) show that Nu behaves in a parabolic way. However, the rate of heat exchange is greater at the lower face (Figure 7(c) of the obstacle than at the top (Figure 7(b) and increases with the Rayleigh number. This is due to the significant decrease in the density of the hot fluid moving upward and the descent of the cold fluid downward below the obstacle

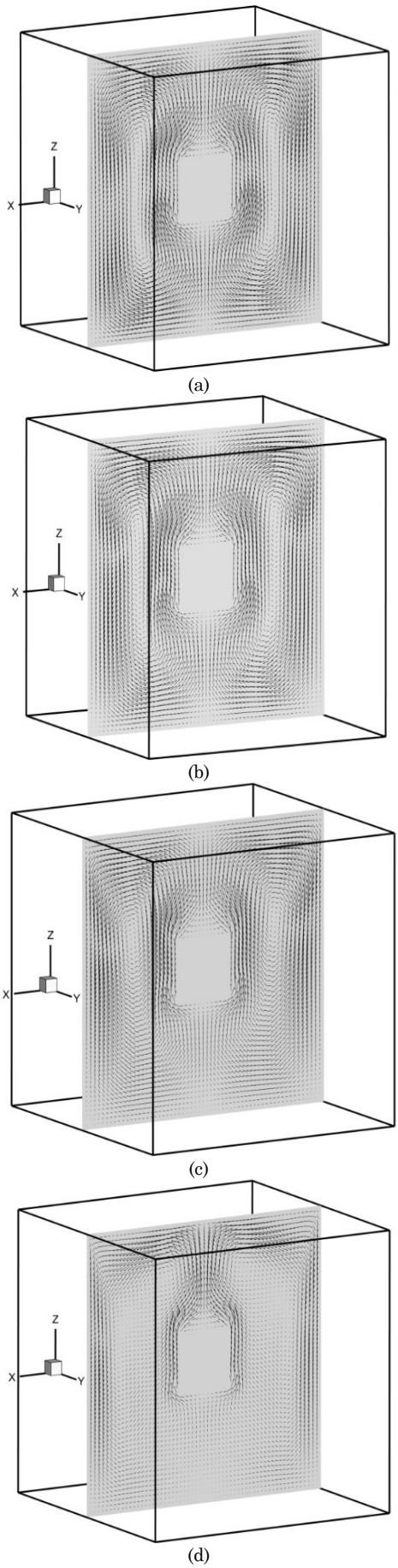

Fig 6. Velocity field plotted at the center plane of the cavity ($\vec{x}, \vec{z}$) for $Ra = 10^3$ (a), 10^4 (b), 10^5 (c) and 10^6 (d).

Thus, the fluid gives up its heat to the lower face of the hot block, and the heat exchange on this face increases. These remarks can be well deduced from Table 3, which gives the average Nusselt number calculated at each face of the obstacle for different Ra values. This table shows that for $Ra = 10^3$, $\langle Nu \rangle$ is almost the same on all faces. This indicates that these faces exchange heat with the cold fluid in the same way. When $Ra \geq 10^4$, the exchange starts to become maximum on the lower face and minimum on the upper one. Table 3 also illustrates $\langle Nu \rangle$ calculated at the four surfaces of the solid. In this case, it can be deduced that the exchange is almost the same for $Ra \leq 10^4$ and increases significantly by augmenting Ra. This is due to the change in the thermal regime of the medium, which passes from a conductive one to a convective one.

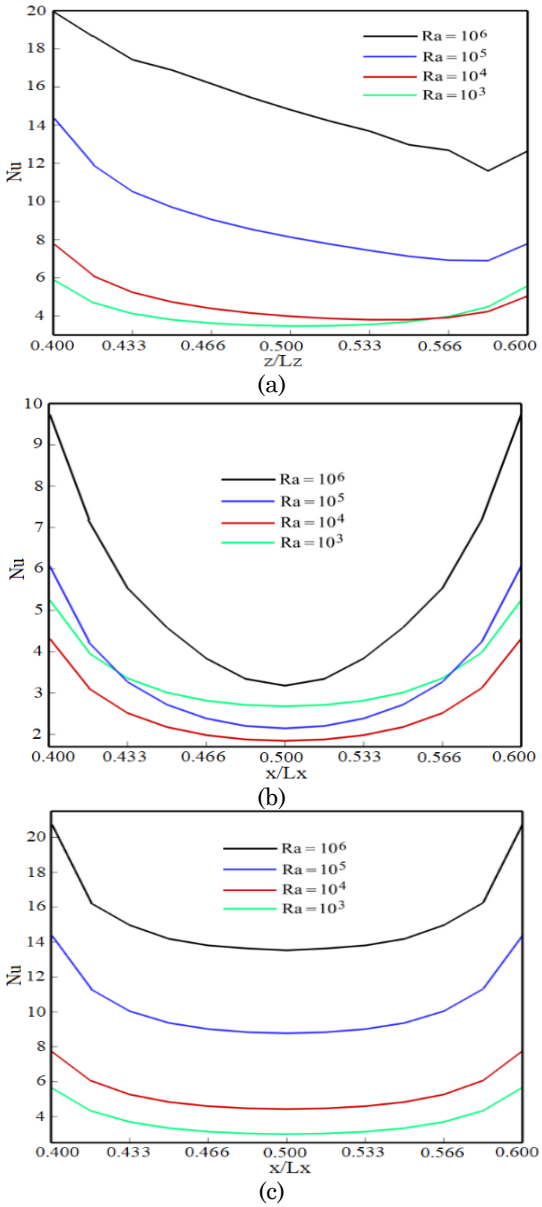

Fig 7: Evolution of Nu calculated at the middle of the left (a), top (b) and bottom (c) faces of the hot obstacle.

Table 3
$\langle N_u \rangle$ calculated in the middle of different faces of the obstacle for various Ra.

Ra	10^3	10^4	10^5	10^6
Left face	0.898	1.016	1.936	3.286
Right face	0.898	1.016	1.936	3.286
Top face	0.748	0.563	0.731	1.193
Bottom face	0.822	1.173	2.243	3.344
Four faces	3.366	3.768	6.46	11.109

4. Conclusions

This paper presented a three-dimensional numerical study of free convection between a hot obstacle and two cold vertical walls of an air-filled cubic cavity. The lattice Boltzmann approach based on the MRT-D3Q19 model has been applied to calculate the velocities and density. The finite-difference technique based on the centered fourth-order scheme was used to calculate the temperature. In a first step, a numerical study focused on the simulation of natural convection inside a differentially heated cubic cavity was performed and considered as a validation of our hybrid numerical approach. Then, the study of the heat exchange between the hot block and the cold walls was considered. Through this study, the temperature and fluid flow behaviors have been discussed. To characterize our numerical study, the average and local Nusselt numbers were calculated. A distinction in the calculation of these dimensionless numbers at each face of the obstacle has been presented. For a low value of Ra ($Ra = 10^3$ for example), the calculations showed that the fluid exchanges its heat almost equally with all the hot surfaces of the obstacle. However, for significant values of Ra ($Ra \geq 10^4$), the results showed that the rate of heat exchange is more important on the lower face of the obstacle compared with the other surfaces.

References

Admi, Y., Moussaoui, M. A., & Mezrhab, A. (2022). Numerical Investigation of Convective Heat Transfer and Fluid Flow Past a Three-Square Cylinders Controlled by a Partition in Channel. *International Journal of Renewable Energy Development,* 11(3), 766-781. doi: 10.14710/ijred.2022.43790

Baïri, A., Zarco-Pernia, E., & De María, J. M. G. (2014). A review on natural convection in enclosures for engineering applications. The particular case of the parallelogrammic diode cavity. *Applied Thermal Engineering,* 63(1), 304-322. doi: 10.1016/j.applthermaleng.2013.10.065

Bejan, A., & Kraus, A. D. (2003). *Heat transfer handbook* (Vol. 1). John Wiley & Sons.

Benhamou, J., Jami, M., Mezrhab, A., Botton, V., & Henry, D. (2020). Numerical study of natural convection and acoustic waves using the lattice Boltzmann method. *Heat Transfer*, 49(6), 3779-3796. doi: 10.1002/htj.21800

Benhamou, J., Jami, M., Mezrhab, A., Henry, D., & Botton, V. (2022). Numerical simulation study of acoustic waves propagation and streaming using MRT-lattice Boltzmann method. *International Journal for Computational Methods in Engineering Science and Mechanics*, 1-14. doi: 10.1080/15502287.2022.2050844

Benhamou, J., & Jami, M. (2022). Three-dimensional numerical study of heat transfer enhancement by sound waves using mesoscopic and macroscopic approaches. *Heat Transfer*. doi: 10.1002/htj.22482

Benhamou, J., Channouf, S., Jami, M., Mezrhab, A., Henry, D., & Botton, V. (2021). Three-Dimensional Lattice Boltzmann Model for Acoustic Waves Emitted by a Source. *International Journal of Computational Fluid Dynamics,* 35(10), 850-871. doi: 10.1080/10618562.2021.2019226

Bettaibi, S., Kuznik, F., & Sediki, E. (2014). Hybrid lattice Boltzmann finite difference simulation of mixed convection flows in a lid-driven square cavity. *Physics Letters A*, 378(32-33), 2429-2435.. doi: 10.1016/j.physleta.2014.06.032

Chorin, P., Moreau, F., & Saury, D. (2020). Heat transfer modification of a natural convection flow in a differentially heated cavity by means of a localized obstacle. *International Journal of Thermal Sciences*, 151, 106279. doi: 10.1016/j.ijthermalsci.2020.106279

D'Humières, D., Ginzburg, I., Krafczyk, M., Lallemand, P., & Luo, L. S. (2002). Multiple–relaxation–time lattice Boltzmann models in three dimensions. *Philosophical Transactions of the Royal Society of London. Series A: Mathematical, Physical and Engineering Sciences*, 360(1792), 437-451. doi: 10.1098/rsta.2001.0955

Fusegi, T., Hyun, J. M., Kuwahara, K., & Farouk, B. (1991). A numerical study of three-dimensional natural convection in a differentially heated cubical enclosure. *International Journal of Heat and Mass Transfer*, 34(6), 1543-1557. doi: 10.1016/0017-9310(91)90295-P

Ghachem, K., Hassen, W., Maatki, C., Kolsi, L., Al-Rashed, A. A., & Naceur, M. (2018). Numerical simulation of 3D natural convection and entropy generation in a cubic cavity equipped with an adiabatic baffle. *International Journal of Heat and Technology*, 36(3), 1047-1054. doi: 10.18280/ijht.360335

Hasnaoui, S., Amahmid, A., Beji, H., Raji, A., Hasnaoui, M., El Mansouri, A., & Alouah, M. (2018). Hybrid lattice Boltzmann finite difference simulation of Soret convection flows in a square cavity with internal heat generation. *Numerical Heat Transfer, Part A: Applications*, 74(1), 948-973. doi: 10.1080/10407782.2018.1487690

Ibrahim, M., Saeed, T., Algehyne, E. A., Alsulami, H., & Chu, Y. M. (2021). Optimization and effect of wall conduction on natural convection in a cavity with constant temperature heat source: Using lattice Boltzmann method and neural network algorithm. *Journal of Thermal Analysis and Calorimetry,* 144(6), 2449-2463. doi: 10.1007/s10973-021-10654-0

Karki, P., Yadav, A. K., & Arumuga Perumal, D. (2019). Study of adiabatic obstacles on natural convection in a square cavity using lattice Boltzmann method. *Journal of Thermal Science and Engineering Applications*, 11(3). doi: 10.1115/1.4041875

Khan, Z. H., Hamid, M., Khan, W. A., Sun, L., & Liu, H. (2021). Thermal non-equilibrium natural convection in a trapezoidal porous cavity with heated cylindrical obstacles. *International Communications in Heat and Mass Transfer,* 126, 105460. doi: 10.1016/j.icheatmasstransfer.2021.105460

Krivovichev, G. V. (2019). Stability analysis of body force action models used in the single-relaxation-time single-phase lattice Boltzmann method. *Applied Mathematics and Computation*, 348, 25-41. doi: 10.1016/j.amc.2018.11.056

Lahmer, E. B., Benhamou, J., Admi, Y., Moussaoui, M. A., Jami, M., Mezrhab, A., & Phanden, R. K. (2022). Assessment of Conjugate and Convective Heat Transfer Performance over a Partitioned Channel within Backward-Facing Step using the Lattice Boltzmann Method. *Journal of Enhanced Heat Transfer,* 29(3), 51-77. doi: 10.1615/JEnhHeatTransf.2022040357

Lallemand, P., & Luo, L. S. (2003). Hybrid finite-difference thermal lattice Boltzmann equation. *International Journal of Modern Physics B*, 17(01n02), 41-47.. doi: 10.1142/s0217979203017060

Lee, J. R. (2018). On the three-dimensional effect for natural convection in horizontal enclosure with an adiabatic body: Review from the 2D results and visualization of 3D flow structure. *International Communications in Heat and Mass Transfer*, 92, 31-38. doi: 10.1016/j.icheatmasstransfer.2018.02.010

Li, Z., Yang, M., & Zhang, Y. (2016). Lattice Boltzmann method simulation of 3-D natural convection with double MRT model. *International Journal of Heat and Mass Transfer*, 94, 222-238. doi: 10.1016/j.ijheatmasstransfer.2015.11.042

Liu, H., Ba, Y., Wu, L., Li, Z., Xi, G., & Zhang, Y. (2018). A hybrid lattice Boltzmann and finite difference method for droplet dynamics with insoluble surfactants. *Journal of Fluid Mechanics*, 837, 381-412. doi: 10.1017/jfm.2017.859

Luo, L. S. (1998). Unified theory of lattice Boltzmann models for

nonideal gases. *Physical review letters*, 81(8), 1618. doi: 10.1103/PhysRevLett.81.1618

Mezrhab, A., Moussaoui, M. A., Jami, M., Naji, H., & Bouzidi, M. H. (2010). Double MRT thermal lattice Boltzmann method for simulating convective flows. *Physics Letters A*, 374(34), 3499-3507. doi: 10.1016/j.physleta.2010.06.059

Minkowycz, W. J., Sparrow, E. M., & Murthy, J. Y. (2000). Handbook of Numerical Heat Transfer, Second Edition. In John Wiley & Sons. doi: 10.1002/9780470172599

Mohamad, A. A. (2019). Lattice Boltzmann Method: Fundamentals and Engineering Applications with Computer Codes: Second Edition. Springer London. doi: 10.1007/978-1-4471-7423-3

Mohamad, A. A., & Kuzmin, A. (2010). A critical evaluation of force term in lattice Boltzmann method, natural convection problem. *International Journal of Heat and Mass Transfer,* 53(5–6), 990–996. doi: 10.1016/j.ijheatmasstransfer.2009.11.014

Nee, A. (2020a). Hybrid lattice Boltzmann—Finite difference formulation for combined heat transfer problems by 3D natural convection and surface thermal radiation. *International Journal of Mechanical Sciences,* 173, 105447. doi: 10.1016/j.ijmecsci.2020.105447

Nee, A. (2020b). Hybrid meso-macroscopic simulation of three-dimensional natural convection combined with conjugate heat transfer. *Thermal Science and Engineering Progress*, 19, 100584.. doi: 10.1016/j.tsep.2020.100584

Nee, A. (2021). Hybrid Lattice Boltzmann Simulation of Three-Dimensional Natural Convection. *Journal of Computational and Theoretical Transport*, 50(4), 280-296. doi: 10.1080/23324309.2021.1942061

Nouni, M., Bendaraa, A., Ouhroum, M., Charafi, M. M., & Hasnaoui, A. (2021). Numerical study of obstacles effect on natural convection inside square cavity: Lattice Boltzmann method. *AIP Conference Proceedings,* 2345(1), 020010. doi: 10.1063/5.0050208

Özişik, M. N., Orlande, H. R., Colaco, M. J., & Cotta, R. M. (2017). *Finite difference methods in heat transfer: Second Edition*. CRC press. doi: 10.1201/9781315121475

Purusothaman, A., Murugesan, K., & Chamkha, A. J. (2019). 3D modeling of natural convective heat transfer from a varying rectangular heat generating source. *Journal of Thermal Analysis and Calorimetry,* 138(1), 597-608. doi: 10.1007/s10973-019-08259-9

Purusothaman, A., Baïri, A., & Nithyadevi, N. (2016). 3D natural convection on a horizontal and vertical thermally active plate in a closed cubical cavity. *International Journal of Numerical Methods for Heat & Fluid Flow*, 26(8), 2528-2542. doi: 10.1108/HFF-08-2015-0341

Rahimi, A., Dehghan Saee, A., Kasaeipoor, A., & Hasani Malekshah, E. (2019). A comprehensive review on natural convection flow and heat transfer: The most practical geometries for engineering applications. In *International Journal of Numerical Methods for Heat and Fluid Flow*. doi: 10.1108/HFF-06-2018-0272

Shan, X., & Chen, H. (1993). Lattice Boltzmann model for simulating flows with multiple phases and components. *Physical Review E,* 47(3), 1815. doi: 10.1103/PhysRevE.47.1815

Shan, X., & Chen, H. (1994). Simulation of nonideal gases and liquid-gas phase transitions by the lattice Boltzmann equation. *Physical Review E,* 49(4), 2941. doi: 10.1103/PhysRevE.49.2941

Shi, Y., Zhao, T. S., & Guo, Z. L. (2006). Finite difference-based lattice Boltzmann simulation of natural convection heat transfer in a horizontal concentric annulus. *Computers and Fluids*, 35(1), 1-15. doi: 10.1016/j.compfluid.2004.11.003

Subhani, S., & Kumar, R. S. (2021). Natural Convection Heat Transfer Enhancement of Circular Obstacle within Square Enclosure. *Journal of Thermal Analysis and Calorimetry*, 1-19. doi: 10.1007/s10973-021-10829-9

Theodore, L. (2011). Heat Transfer Applications for the Practicing Engineer. John Wiley & Sons. doi: 10.1002/9780470937228

Ugurlubilek, N., Sert, Z., Selimefendigil, F., & Öztop, H. F. (2022). 3D laminar natural convection in a cubical enclosure with gradually changing partitions. *International Communications in Heat and Mass Transfer*, 133, 105932. doi: 10.1016/j.icheatmasstransfer.2022.105932

Vesper, J. E., Tietjen, S. C., Chakkingal, M., & Kenjereš, S. (2022). Numerical analysis of effects of fins and conductive walls on heat transfer in side heated cavities — Onset of three-dimensional phenomena in natural convection. *International Journal of Heat and Mass Transfer*, 183, 122033. doi: 10.1016/j.ijheatmasstransfer.2021.122033

Wang, P., Zhang, Y., & Guo, Z. (2017). Numerical study of three-dimensional natural convection in a cubical cavity at high Rayleigh numbers. *International Journal of Heat and Mass Transfer,* 113, 217-228. doi: 10.1016/j.ijheatmasstransfer.2017.05.057

Xiong, P. Y., Hamid, A., Iqbal, K., Irfan, M., & Khan, M. (2021). Numerical simulation of mixed convection flow and heat transfer in the lid-driven triangular cavity with different obstacle configurations. *International Communications in Heat and Mass Transfer*, 123, 105202. doi: 10.1016/j.icheatmasstransfer.2021.105202

Xu, A., Gonnella, G., & Lamura, A. (2006). Simulations of complex fluids by mixed lattice Boltzmann - Finite difference methods. *Physica A: Statistical Mechanics and Its Applications,* 362(1), 42-47. doi: 10.1016/j.physa.2005.09.015

Yousif, A. A., Alomar, O. R., & Hussein, A. T. (2022). Impact of using triple adiabatic obstacles on natural convection inside porous cavity under non-darcy flow and local thermal non-equilibrium model. *International Communications in Heat and Mass Transfer,* 130, 105760. doi: 10.1016/j.icheatmasstransfer.2021.105760